

# Structural Applications of Ferritic Stainless Steels (SAFSS)

WP 3.5 Heat transfer characteristics of  
ferritic stainless steel decking

Report To RFCS  
Document: RT1561  
Version: 02  
Date: March 2012

Version	Issue	Purpose	Author	Reviewer	Approved
01		Draft Feb 2012	JAL	KAC	NRB
02		Final March 2012	JAL	KAC	NRB

Although all care has been taken to ensure that all the information contained herein is accurate, The Steel Construction Institute assumes no responsibility for any errors or misinterpretations or any loss or damage arising therefrom.

For information on publications, telephone direct: +44 (0) 1344 636505  
or Email: [publications@steel-sci.com](mailto:publications@steel-sci.com)

For information on courses, telephone direct: +44 (0) 1344 636500  
or Email: [education@steel-sci.com](mailto:education@steel-sci.com)

Email: [reception@steel-sci.com](mailto:reception@steel-sci.com)

World Wide Web site: <http://www.steel-sci.org>

## EXECUTIVE SUMMARY

Thermal mass of composite slabs may be utilised over a daily heating cycle by releasing and absorbing heat to and from the room space below. By absorbing heat during the day and releasing the heat by night, when the temperature outside the slab drops, large fluctuations in room temperature may be avoided. This inherent passive heating and cooling system can provide an effective means of thermoregulation within an environment.

This report describes an investigation into the heat transfer characteristics of ferritic stainless steel decking in a composite floor slab. The thermal response was studied for a range of decks thicknesses, concrete thicknesses, profile shape and surface emissivity. Comparisons were also made with galvanised steel decking and a concrete slab with no decking.

When the deck thickness was varied, within reasonable limits, there was no significant increase in thermal flux across the surface. When the concrete thickness was varied, the thermal flux increased until the concrete thickness reached a certain depth (140 mm approximately), after which there was no significant increase in thermal flux across the bottom surface.

When the profile shape was varied, the thermal flux changed significantly. On further investigation it was found that this was predominantly due to the different quantities of concrete used for the four profile shapes. When this difference in concrete volume was accounted for, it was found that the three metal deck profiles appeared to be very similar in their “effectiveness” at transferring heat to the slab. The 200 mm flat slab was found to be considerably less effective at transferring heat due to the smaller surface area of the concrete slab.

When the emissivity of the surface increased, the thermal flux increased: the shinier the surface (i.e. the lower the emissivity), the less effective the surface at transferring heat to the slab.

Integrating the values obtained for admittance and transmittance into the simplified model of the CIBSE Guide A Example 5.2, it was found that although the values of admittance and transmittance vary between a 130 mm thick slab with ferritic stainless steel decking, a 130 mm thick slab with galvanised steel decking and 200 mm concrete slab, the three models were all categorised as having a ‘slow thermal response’. This leads to the conclusion that buildings with these floor systems will have the same solar gain factor and ultimately will result in the same values being calculated for mean and peak operative temperature.



## Contents

	Page No
EXECUTIVE SUMMARY	iii
1 Introduction	1
1.1 The use of thermal mass to regulate building temperature	1
1.2 Heat transfer mechanisms in composite floors	2
1.3 Scope of WP3.5	4
2 Calibration of the thermal Model	5
2.1 Properties of the models	5
2.2 Calibration of the models	6
3 Thermal analysis of composite floors with ferritic stainless steel decking	11
3.1 Introduction	11
3.2 Variation in deck thicknesses	12
3.3 Variation in concrete thicknesses	14
3.4 Variation in profile shape	16
3.5 Variation in emissivity	20
4 Impact on whole building energy performance	22
4.1 Calculation of thermal admittance and thermal transmittance	22
4.2 CIBSE simplified model	24
5 Conclusions	26
6 Recommendations for further work	27
7 References	28



# 1 INTRODUCTION

## 1.1 The use of thermal mass to regulate building temperature

It is increasingly important to design low-energy, sustainable structures. The significant energy efficiency and thermal comfort advantages offered by exploiting the thermal mass in buildings have led to its greater significance in design in the last ten years.

Thermal mass (or thermal capacity) is the ability of a material within the fabric of a building to absorb, store and release heat energy and reduce the energy normally required for cooling. It is measured in the number of Joules of thermal energy stored per unit of mass ( $J/kgK$ ) or per cubic metre of material ( $J/m^3K$ ). The other key parameter is thermal inertia which is a measure of how quickly the temperature responds to changes in heat gain or loss. An increase in thermal inertia is desirable as it results in less fluctuation of the internal temperature thus limiting a building's response to external conditions (i.e. weather) and also internal losses and gains. Knowledge and consideration of these issues can enable engineers to design buildings without mechanical cooling systems and hence with lower carbon emissions.

Typically, the most influential and useful structural components contributing to thermal mass are floor and ceiling slabs. Walls are usually rather lightweight and therefore have little useful thermal mass. Exposing the surfaces of floor slabs allows the structural mass to interact thermally with the internal environment, thereby increasing the thermal inertia of the occupied spaces.

Floor slabs absorb excess heat during the day, thus avoiding or reducing overheating. At night, the cooler ambient air is used to ventilate the internal spaces and cool the slabs, removing the heat stored during the previous day and preparing the slabs for absorbing further thermal energy the following day. This can reduce or eliminate the mechanical cooling load in many buildings in summer and is particularly useful in office buildings, which tend to make high thermal gains from occupants, computers and other equipment, lighting and glazed facades. Figure 1-1 illustrates this concept, and Figure 1-2 shows how thermal mass strategies work; both are taken from Reference [1].

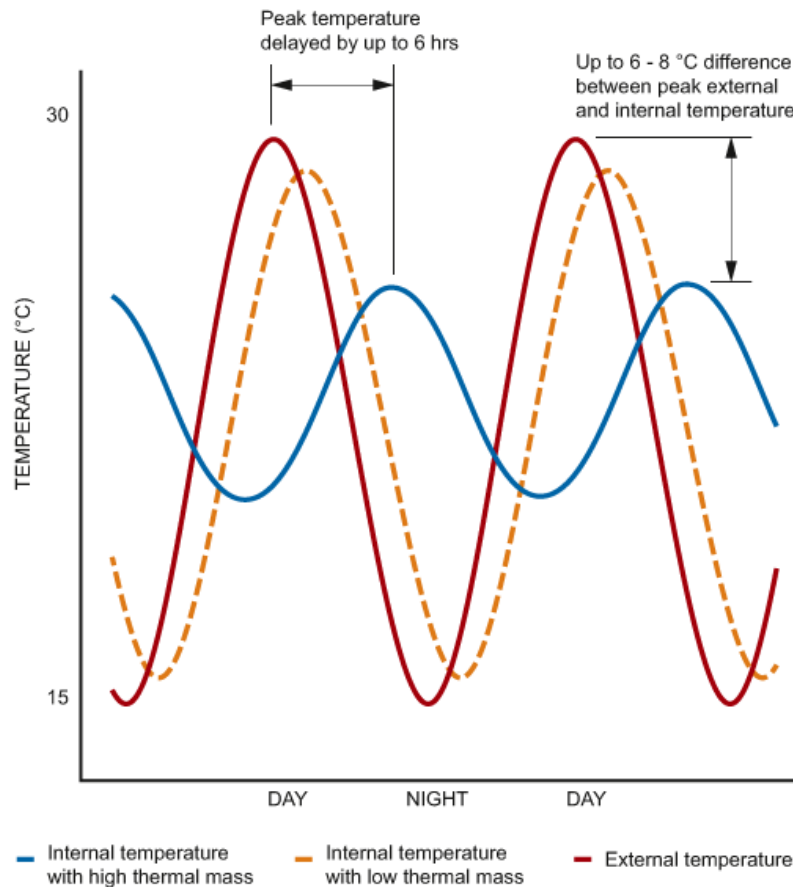


**Figure 1-1** Effects of thermal mass on internal temperatures

## 1.2 Heat transfer mechanisms in composite floors

Figure 1-3 shows typical composite deck profiles and their slab depths. Thermal modelling using tools such as TRNSYS, TAS and ANSYS have been used to simulate the thermal characteristics of composite floors and have concluded that the thermal capacity of composite floors is governed by the surface heat transfer characteristics, rather than the depth or volume of the concrete slabs.

It has been found that there is little benefit from increasing the slab thickness above approximately 100 mm, as it is the rate at which heat can be absorbed into the fabric that is the limiting factor for how much thermal energy can be stored <sup>[2]</sup>. For typical concrete floor construction types used in both steel and concrete frame office buildings, the capacity of the slab to store the thermal energy is superior to the rate of surface heat transfer over a 24-hour cycle and therefore relatively deep slabs are of little benefit in this respect.

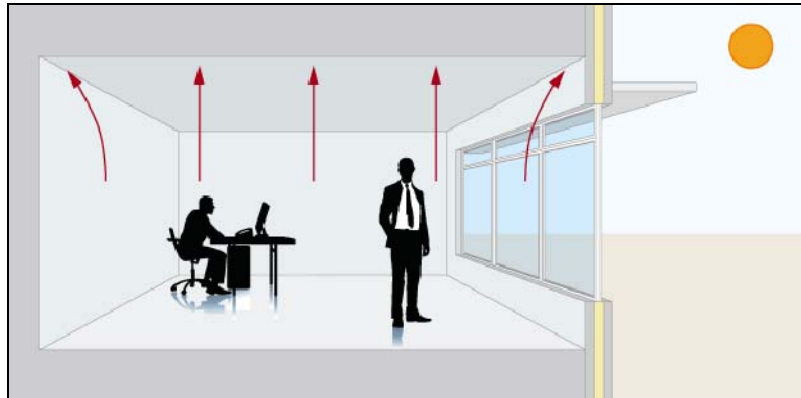
The total heat transfer is a combination of the heat transferred through convection as well as radiation. Improvements in surface heat transfer can be achieved by increasing the surface area through the formation of coffers, troughs, or profiling the surface such as is the case for composite deck floor slabs. This is because the radiation component is dependent on the shape of the deck profile and the emissivity of the surfaces. Typically, profiled decks can approximately double the exposed underside surface area and hence the heat transfer; this is likely to be more relevant than increasing the mass.



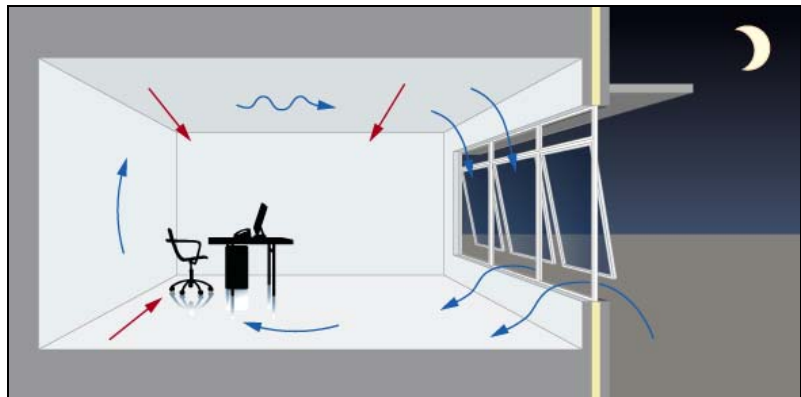
During the day, heat is produced in the building from solar gains, human activity and electrical equipment



The warm air rises and is absorbed by the thermal mass in the exposed surfaces of the walls and upper floors



At night, cool air ventilates the building, purging heat from the fabric



This process is repeated on a diurnal or daily basis during hot weather.

**Figure 1-2 How thermal mass strategies work**

ISO 6946 <sup>[3]</sup> uses a heat transfer of  $5 \text{ W/m}^2\text{K}$  for heat transfer into the slab (in the heating cycle), but only  $0.7 \text{ W/m}^2\text{K}$  for heat transfer out of the slab during cooling. The difference is due to the natural air movement and thermal contact between the room area and the slab surface. In addition, the vertical faces are less efficient in terms of heat transfer than horizontal faces. Two faces of trapezoidal deck profiles are almost vertical, and so their heat transfer coefficient is reduced. There are also several special profiles with narrow re-entrant ribs (such as Holorib), in which the convective heat transfer will be reduced due to the limited air contact with the rib.

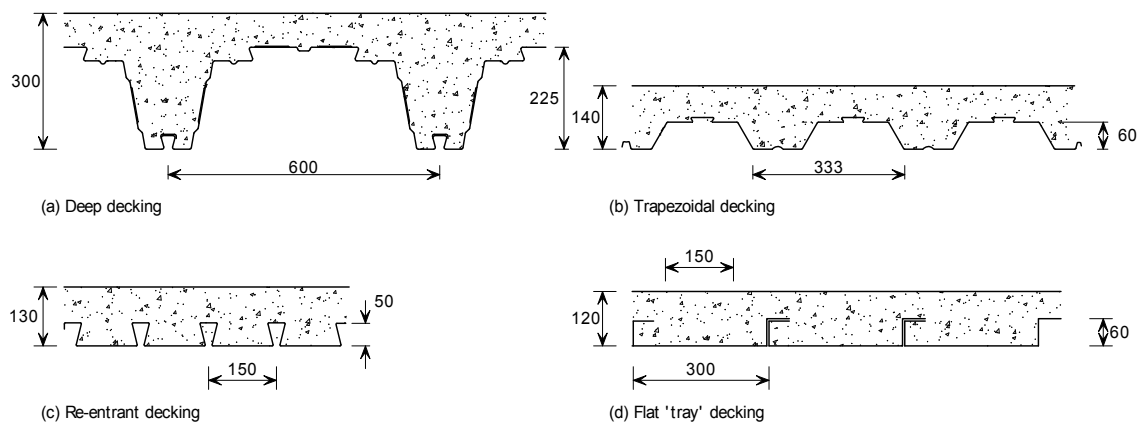


**Figure 1-3 Typical composite slab profiles**

It is important to note that research has shown that the presence of false ceilings, carpets or floor voids may considerably reduce the heat transfer to the slab. This is because they effectively insulate the composite floor from the internal environment. Therefore, in order to utilise the thermal capacity of the composite floor, the steel decking needs to be exposed. If this is not desirable, it may be possible to use solid drop ceilings if they are made from a conducting material rather than an insulating material. Alternatively, designers might employ partial false ceilings or perforated ceiling tiles. This permits air to circulate between the ceiling void and space below, making direct use of convective heat transfer. Research suggests that as little as 15% open area is sufficient to allow significant air circulation and heat transfer<sup>[4]</sup>.

Another important point about utilising the concrete slab as thermal mass is that this can increase the service costs during winter months as the additional heat required to heat the building might increase the energy demand by 10-20%. During winter, when mechanical heating is typically used, a relatively large thermal mass will lose heat at a comparatively slow rate when the heating is switched off. However, on the other hand, it also takes longer to heat up the space when heating is turned back on. This issue is intensified if the building is poorly insulated. Engineers need to exercise care and consideration when designing buildings, particularly in relation to the materials employed, as the balance between the reduction in cooling demand and the increase in heating demand is complex and will vary between buildings.

### 1.3 Scope of WP3.5

The main objective of Task 3.5 is to establish if composite slabs comprising ferritic decking can provide a means of passively cooling a building in the summer, thereby reducing the need for expensive air conditioning. In order to do this, a transient thermal analysis of composite ferritic stainless steel decking using Finite Element Analysis (FEA) will be carried out and the performance of ferritic decking compared to that of galvanised steel decking and a solid concrete slab. Finally, the performance of the exposed composite slab as part of a whole building energy model will be evaluated in order to establish the reduction in heating / cooling demand for the building.

## 2 CALIBRATION OF THE THERMAL MODEL

### 2.1 Properties of the models

ANSYS Mechanical 13 software was used in this analysis. The models were calibrated against previous work by Oxford Brookes University and Corus <sup>[5,6,7]</sup>. Two models were used in this calibration exercise: the first was a simple 200 mm flat concrete slab and the second a “Deep deck” galvanised steel profile. Table 2-1 gives the material properties assumed in the models. The boundary conditions were as given in Table 2-2 and Figure 2-1. The properties of the insulation used on the top surface of the concrete slab to represent soft finishing on the floor are given in Table 2-3.

**Table 2-1 Material properties from EN 1994-1-2 <sup>[8]</sup>**

Property			Concrete	Galvanised Steel
Density	$\rho$	kg/m <sup>3</sup>	2300	7850
Specific Heat Capacity	$C_p$	J/kgK	1000	600
Thermal Conductivity	$k$	W/mK	1.6	45

**Table 2-2 Input temperature data <sup>[5]</sup>**

Surface	Insulated	Input Temp	Aver. Temp	Amplitude	Period	Surface Resistance
			°C	°C	hrs	
Top Surface	Yes	Constant	20	-	-	0.13
Bottom	No	Cyclic	22	4	24	0.13

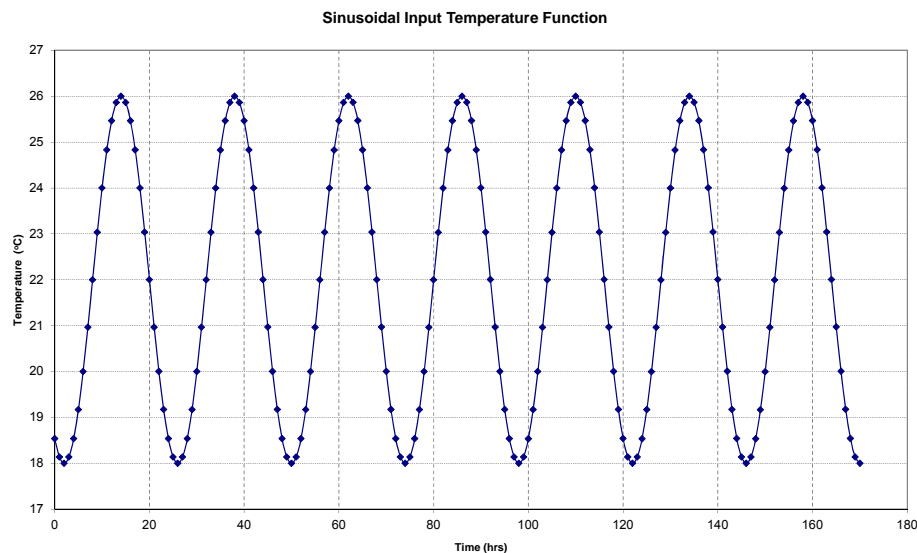


**Figure 2-1 Temperature input at bottom surface (°C)**

**Table 2-3 Assumed Insulation material properties**

50mm thickness			Insulation
Density	$\rho$	kg/m <sup>3</sup>	30
Specific Heat	$C_p$	J/kgK	1170
Thermal Conductivity	$k$	W/mK	0.029

It should be noted that when loads were applied to surfaces in the model a simplified approach was used. This was a similar approach to that used in Reference 5 where surface resistance was assumed to be 0.13m<sup>2</sup>K/W. The loads were applied as convection loads with the film coefficient ( $h$ ) equal to the inverse of the surface resistance. The surface resistance term  $R_s$  is composed of two coefficients  $h_c$  and  $h_r$  : expressions for these parameters are given below <sup>[9]</sup>:

$$R_s = \frac{1}{h_c + h_r}$$

$$h_r = \varepsilon h_{r0}$$

$$h_{r0} = 4\sigma T_m^3$$

Where:

$h_c$  is the convection coefficient

$h_r$  is the radiation coefficient

$\varepsilon$  is the hemispherical emissivity of the surface

$h_{r0}$  is the radiative coefficient for a black-body surface in W/(m<sup>2</sup>K)

$\sigma$  is the Stefan-Boltzmann constant [ $5.67 \times 10^{-8}$  W/(m<sup>2</sup>K<sup>4</sup>)]

$T_m$  is the mean thermodynamic temperature of the surface and of its surroundings, in Kelvin.

## 2.2 Calibration of the models

### 2.2.1 Results from ANSYS

Figure 2-2 shows the nodal temperature profile across the concrete slab and Figure 2-3 shows the nodal thermal flux on the bottom surface over a 7 day cycle. Figure 2-4 and Figure 2-5 gives equivalent results for the deep deck composite slab.

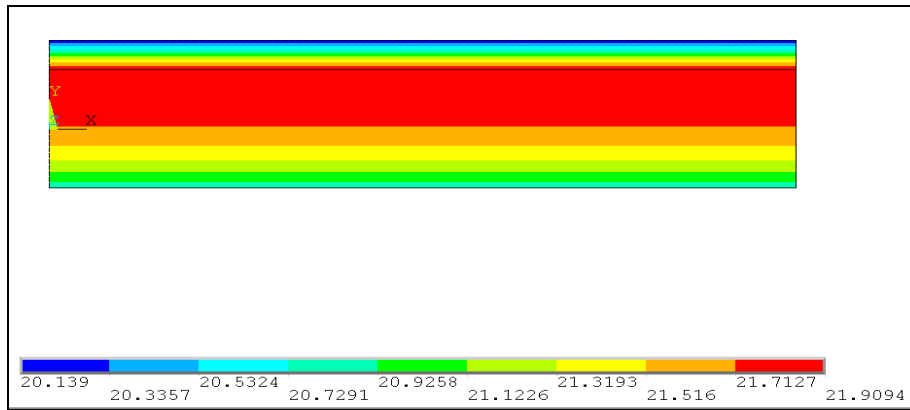


Figure 2-2 Nodal temperature profile (°C) at 3 am in a 200 mm deep concrete slab.

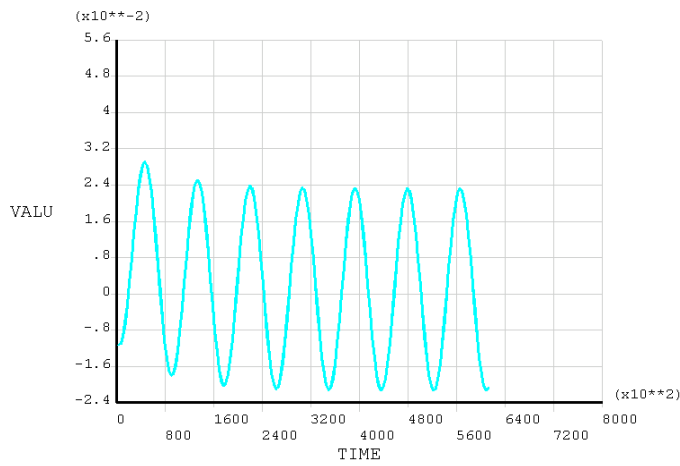


Figure 2-3 Nodal thermal flux (y-axis) on bottom surface (mW/mm<sup>2</sup>). (Time is given on the x-axis in secs. 800x10<sup>2</sup> seconds = 22 hours)

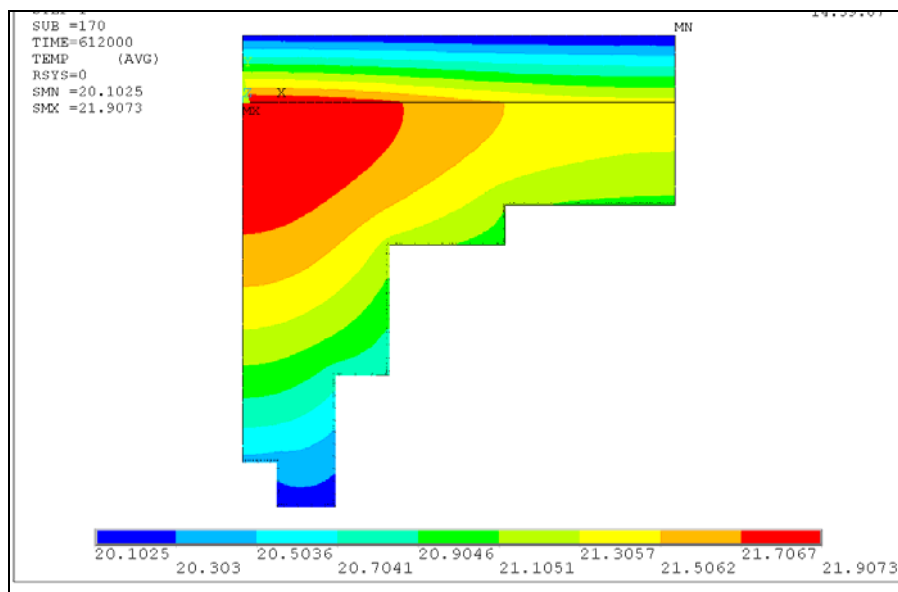
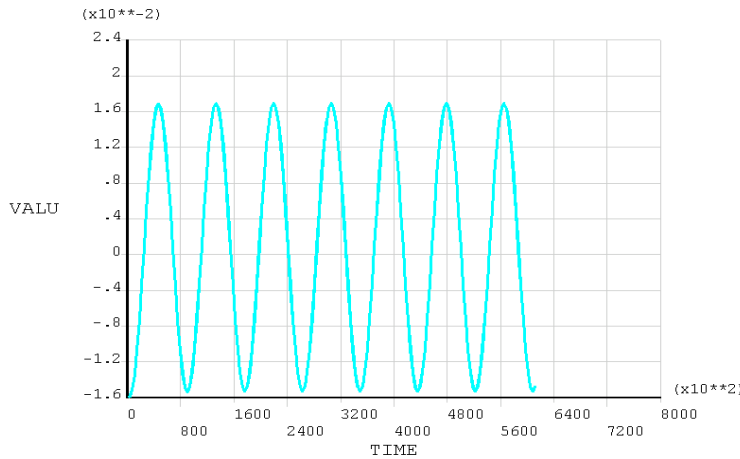


Figure 2-4 Nodal temperature profile (°C) at 3am in a deep deck galvanised steel profile.



**Figure 2-5 Nodal thermal flux (y-axis) on bottom surface of rib (mW/mm<sup>2</sup>).**  
 (Time is given on the x-axis in secs.  $800 \times 10^2$  seconds = 22 hours)

It was noted that the output obtained from ANSYS was in the format of nodal solutions. Reference 5 reports average values across the bottom surface of the model. It was therefore necessary to adjust the values obtained from ANSYS to obtain an average value for the entire bottom surface. This was done by the following method:

The total surface was subdivided into nine separate surfaces, 5 horizontal and 4 vertical (Figure 2-6). A value for thermal flux across each surface was obtained at a central node on that surface. These values were then weighted according to the ratio of the individual surface length to the total surface length of the model. An average value was determined for each load step.

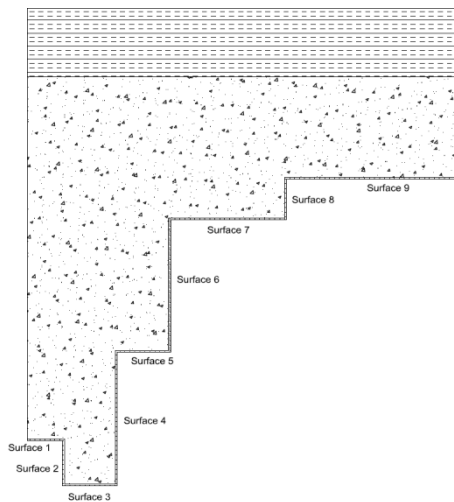


**Figure 2-6 Division of surface to obtain an average thermal flux**

The results for each surface are shown in Figure 2-7, Figure 2-8 and Figure 2-9. The values in Figure 2-7 are for individual nodes, one on each surface. These results were then weighted in the ratio of individual line length to total bottom surface length. The combined results are plotted in Figure 2-8. The results in Figure 2-8 were then multiplied by a factor of 1.86, the ratio of the total surface length of the decking to the horizontal plan length. The 1.86 factor converts the total flux through the deck surface to a flux through a single plane (i.e. horizontal plan area), shown in Figure 2-9.

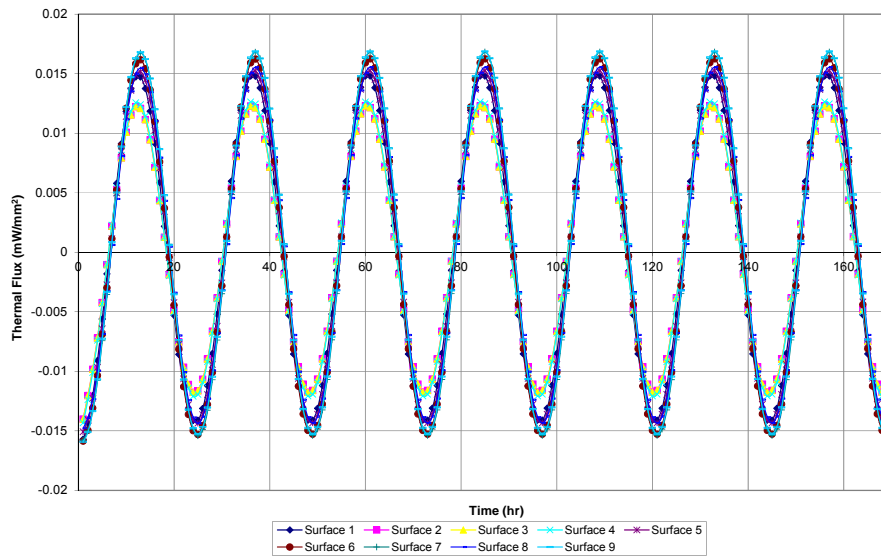


**Figure 2-7 Nodal thermal flux on individual surfaces of deep deck profile (mW/mm<sup>2</sup>)**

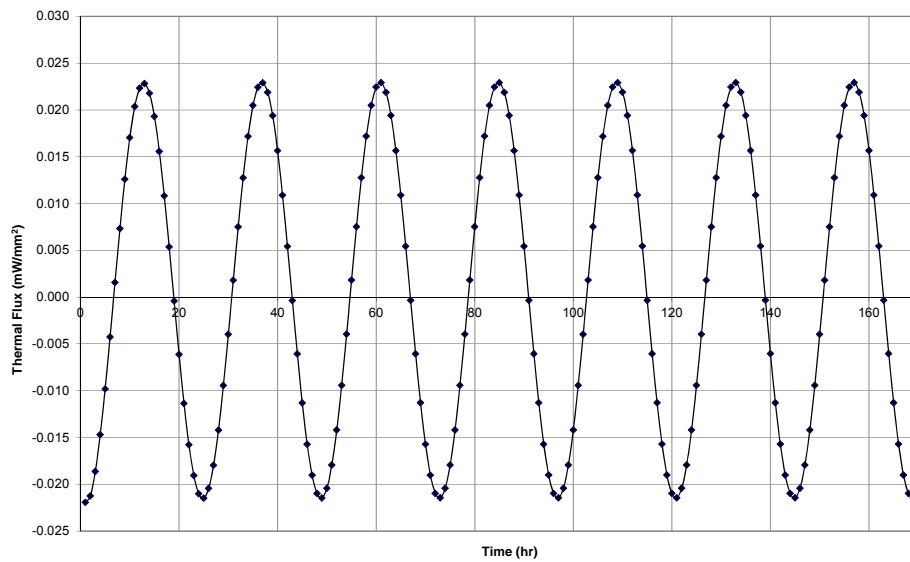


**Figure 2-8 Average nodal thermal flux on bottom surface (mW/mm<sup>2</sup>)**

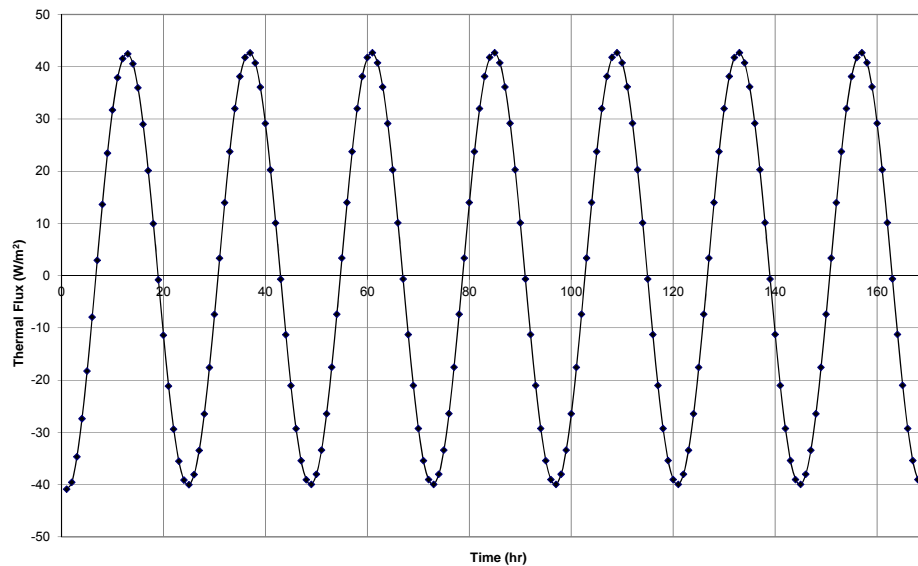


**Figure 2-9 Average thermal flux on bottom surface ( $\text{W/m}^2$ ) (horizontal width of slab)**

## 2.2.2 Comparison of results obtained with those in Reference 5

Table 2-4 compared the results from ANSYS with those in Reference 5.

**Table 2-4 Comparison of results obtained using ANSYS with those of Reference 5**

Description	Ref.[1] Peak Heat Flow ( $\text{W/m}^2$ )	ANSYS Peak Heat Flow ( $\text{W/m}^2$ )
200mm Flat Slab	23.71	23.23
Deep deck	37.35	42.6

The differences in the values can be accounted for as follows:

1. The material properties in the two models may have been slightly different, e.g. the density and specific heat capacities of concrete, steel and insulation were not explicitly given in Reference 5. Also the thickness of insulation and the thermal conductivity of the insulation were not given in Reference 5 and were assumed to be the values given in Table 2-3.
2. At the top surface, the gas temperature is  $20^\circ\text{C}$ , which creates a net temperature differential between the top and bottom surface, where the mean temperature is taken as  $22^\circ\text{C}$ . This temperature differential causes a net heat flow out of the slab through the top surface. The quantity of this flow depends on the temperature differences between the top and bottom surfaces and the properties of the materials the heat flows through. As mentioned above, the properties of the insulation material used on top of the slab in Reference 5 were not known. The values chosen for the ANSYS model appear to provide less insulation than those used in Reference 5. The reduction in insulation provided by the ANSYS model results in a larger heat flow through the top surface. This explains why the offset of the graph of thermal flux from zero for the ANSYS model is greater than that in Reference 5.



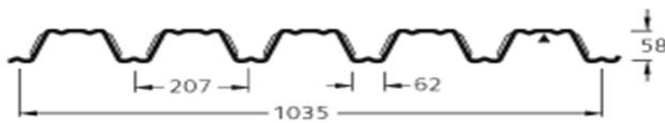
## 3 THERMAL ANALYSIS OF COMPOSITE FLOORS WITH FERRITIC STAINLESS STEEL DECKING

### 3.1 Introduction

Table 3-1 gives the material properties used in the thermal analyses and Figure 3-1 shows the decking profile used in the analysis, which was a ArcelorMittal Cofraplus 60 profile.

**Table 3-1 Material properties for concrete and steel taken from EN 1994-1-2[8] and stainless steel from EN 10088-1[10]**

			Concrete	Galvanised Steel	Grade 1.4003 ferritic Stainless Steel
<b>Density</b>	$\rho$	kg/m <sup>3</sup>	2300	7850	7700
<b>Specific Heat Capacity</b>	$C_p$	J/kgK	1000	600	430
<b>Thermal Conductivity</b>	$k$	W/mK	1.6	45	25
<b>Emissivity</b>	$\varepsilon$		N.A	0.28	0.4



	MAX			kg
	12,00	1500	0,75	0,0877
			0,88	0,1029
			1,00	0,1170

**Figure 3-1 ArcelorMittal Cofraplus 60: profile shape**

The emissivity is a measure of a material's radiating efficiency. An emissivity of 1.0 implies that a material is 100% efficient at radiating energy. Values of emissivity depend on surface roughness and finish. It is therefore difficult to give precise values for materials like stainless steel which can be produced in many different surface finishes. Table 3-2 gives some values taken from three references. The variation in thermal performance as a function of emissivity was studied in Section 3.5. For the other studies reported in Sections 3.2, 3.3 and 3.4, a value of 0.4 was used for stainless steel, which is an average value indicated by the references considered.

**Table 3-2 Values for emissivity for steel and carbon steel**

	Value of emissivity	Reference
<b>Stainless steel</b>		
Polished stainless steel	0.10 - 0.15	11
Oxidized stainless steel	0.45 - 0.95	11
Stainless steel	0.59	12
Stainless plate	0.34	12
Stainless steel, weathered	0.85	13
Stainless steel, polished	0.075	13
Stainless steel type 301	0.54-0.63	13
<b>Steel</b>		
Unoxidized	0.10	11
Oxidized	0.70 - 0.95	11
Cold Rolled	0.70 - 0.90	11
Ground sheet	0.40 - 0.60	11
Rough surface	0.95	11
Steel rolled freshly	0.24	12
Steel oxidised	0.79	13
Steel polished	0.07	13
Galvanised steel	0.28	12
Galvanised steel - old	0.88	13
Galvanised steel - new	0.23	13

### 3.2 Variation in deck thicknesses

The first investigation studied the impact of the thickness of the deck profile on the thermal response of the floor. Four thicknesses of 0.75 mm, 0.88 mm, 1.00 mm and 1.25 mm were chosen. Although a 1.25 mm thick profile is not produced for Cofraplus 60, it is included in the analysis to increase the scope of the finite element analysis test results. The slab depth from trough to top surface was set at 100 mm with a layer of 50 mm insulation covering the top surface. For insulation properties refer to Table 2-3.

Figure 3-2 shows the thermal flux on the bottom surface per horizontal metre for galvanised steel and ferritic stainless steel decking of varying thickness. Figure 3-3 shows the thermal flux on the bottom surface per horizontal metre for galvanised steel and ferritic stainless steel deck for various deck thicknesses. Table 3-3 shows the peak and average thermal flux values for various deck thicknesses.

Table 3-3 shows that the deck thickness does not seem to affect the thermal flux across the surface; this applies to both to the galvanised steel decking and the ferritic stainless steel decking. This can be explained because as the steel decking is extremely thin and has a high thermal conductivity, relative to the concrete above it, the concrete is the dominant material in controlling the thermal flux across the bottom surface. As the quantity and geometry of the concrete was held constant, varying the steel thickness yields little increase in the thermal flux of the system.

There is a noticeable difference between the values obtained for the galvanised steel decking and those of the ferritic stainless steel decking. This is due to the difference in emissivity of the two metals (this is discussed further in Section 3.5).

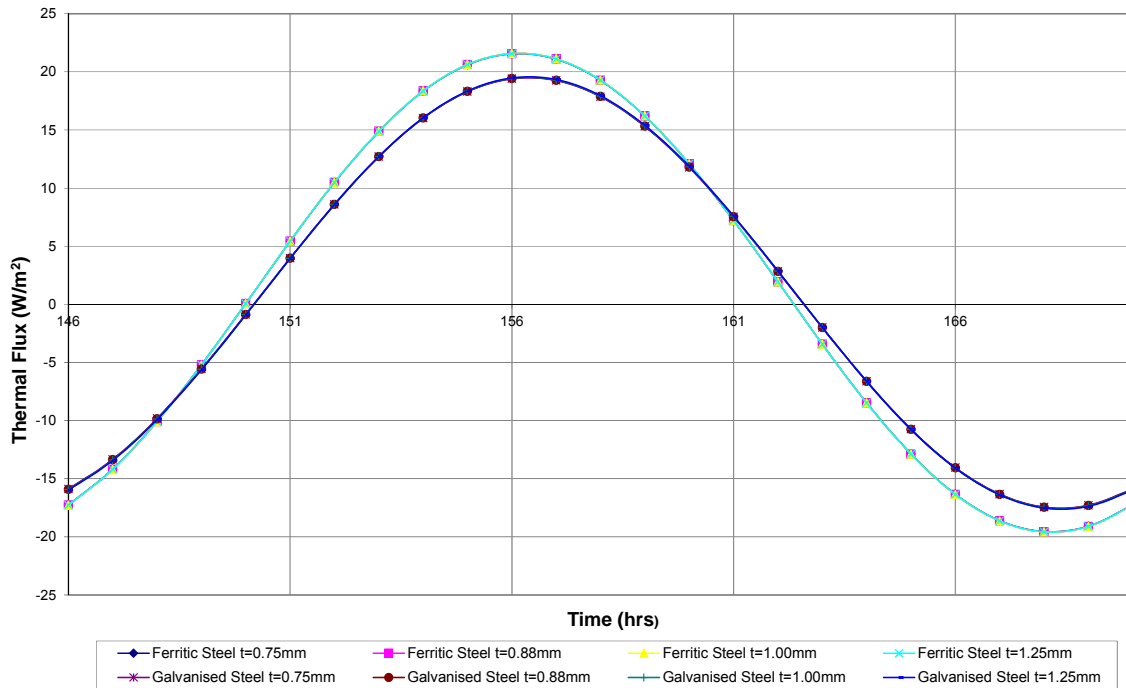


Figure 3-2 7<sup>th</sup> day thermal flux on bottom surface per horizontal metre for galvanised steel and ferritic stainless steel deck ( $W/m^2$ ).



Figure 3-3 Thermal flux ( $W/m^2$ ) on bottom surface per horizontal metre for galvanised steel and ferritic stainless steel deck for various deck thicknesses.

**Table 3-3 Peak and average thermal flux values (8am-5pm) (W/m<sup>2</sup>)**

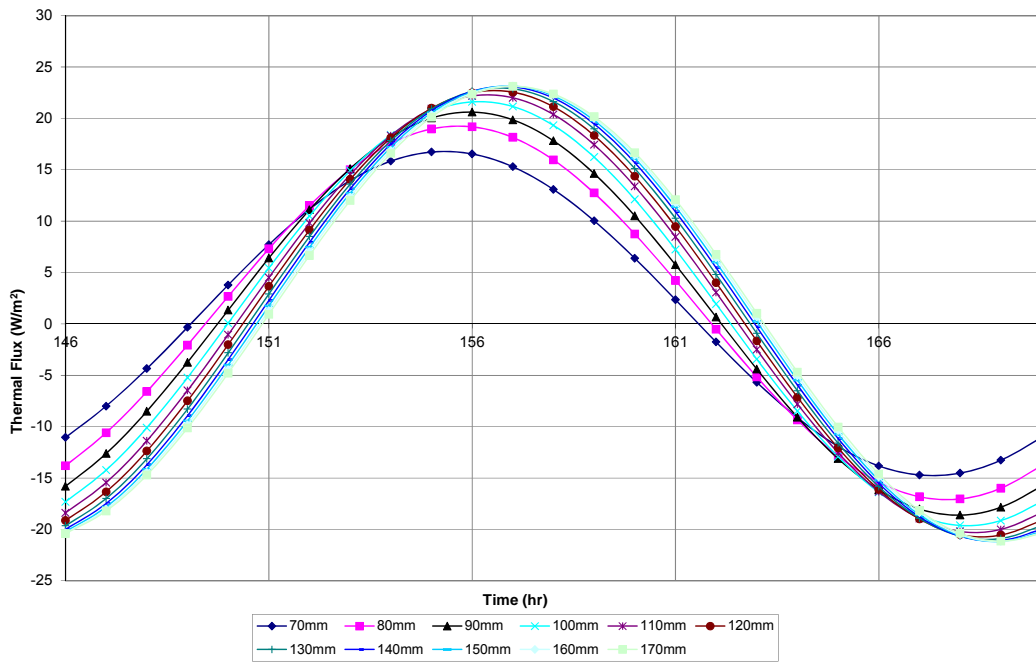
		Deck Thickness			
		0.75mm	0.88mm	1.0mm	1.25mm
Ferritic Stainless Steel Decking	Peak Flux Across 1m Horizontal	21.56	21.57	21.59	21.61
	Average Flux Across 1m Horizontal	16.17	16.18	16.2	16.21
Galvanised Steel Decking	Peak Flux Across 1m Horizontal	19.4	19.43	19.45	19.48
	Average Flux Across 1m Horizontal	14.68	14.7	14.71	14.74

### 3.3 Variation in concrete thicknesses

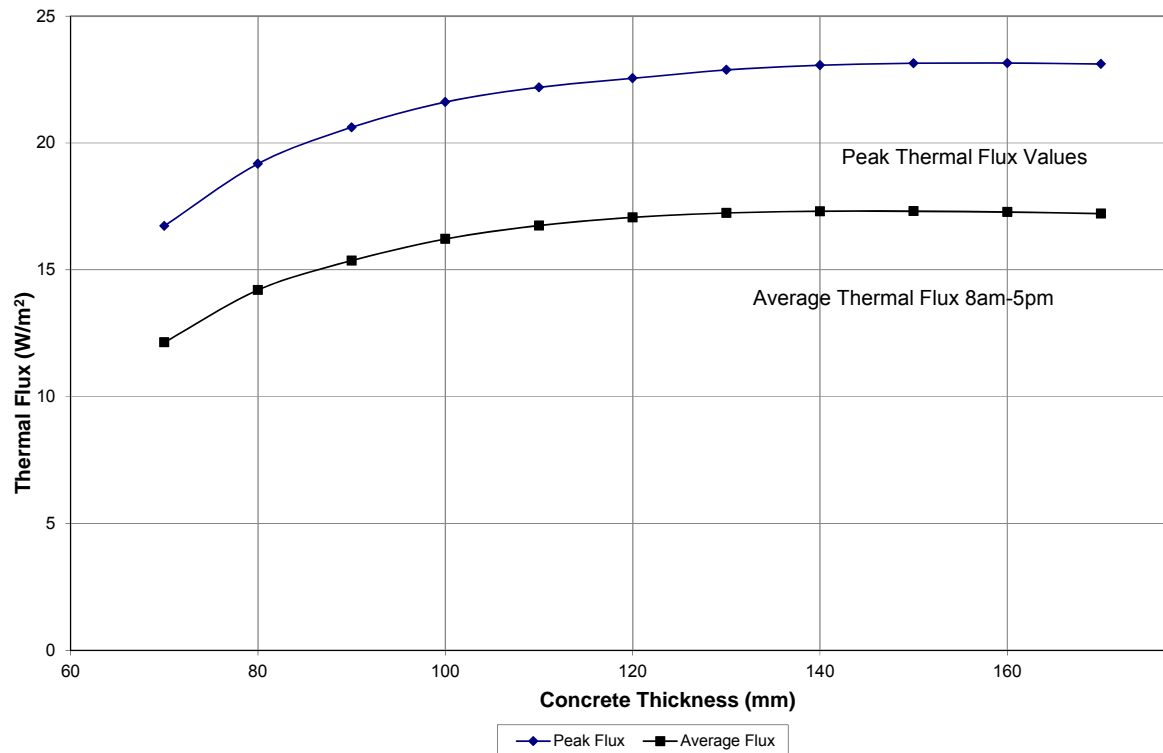
Thermal analyses were carried out using ANSYS to determine the effects of concrete thickness on the thermal response of a composite slab with ferritic stainless steel decking. The deck thickness was 1.25 mm and remained constant for all thermal analyses. Insulation of thickness 50 mm was used across the top surface to represent soft finishing on the floor. Material properties were those given in Table 3-1. The concrete thicknesses studied were from 70 mm to 170 mm in 10 mm increments.

Figure 3-4 shows the thermal flux on the bottom surface per horizontal metre for ferritic stainless steel decking with concrete slabs of varying thicknesses. Figure 3-5 shows the thermal flux on the bottom surface for various concrete thicknesses.

As can be seen from Figure 3-4, as the concrete thickness increases, so does the thermal flux. It is worth noting that once the concrete thickness reaches a certain value, there is no significant increase in thermal flux. This can clearly be seen in Figure 3-5: when the concrete thickness reaches about 120 mm, changes in thermal flux are very slight. Certainly, once the slab thickness reaches 150 mm, there is no significant increase in the thermal flux observed. Figure 3-4 also shows that as the concrete thickness increases, the slab reaches its peak flux later in the day.



**Figure 3-4** 7<sup>th</sup> day thermal flux on bottom surface per horizontal metre for ferritic stainless steel deck ( $W/m^2$ ) and for various concrete thicknesses.



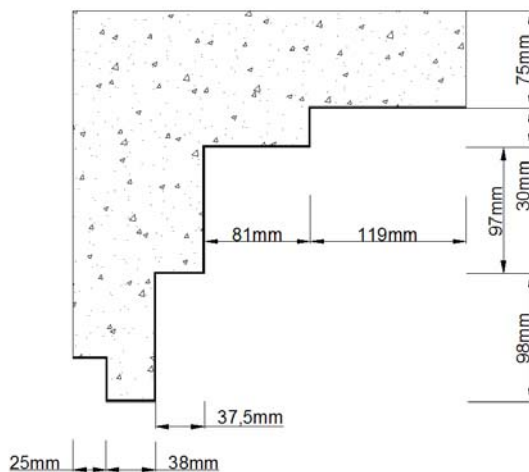
**Figure 3-5** Thermal flux (Peak & Average 8am-5pm) ( $W/m^2$ ) on bottom surface per horizontal metre for ferritic stainless steel deck and various concrete thicknesses

### 3.4 Variation in profile shape

Thermal analyses were carried out to determine the effects of profile shape on the thermal capacity of a composite slab with ferritic stainless steel decking. The following profiles were studied:

- ArcelorMittal Cofraplus 60 (trapezoidal profile),
- Dovetail re-entrant profile with an equal area of concrete to that of the Cofraplus 60 profile (i.e. the diagonal of the Cofraplus 60 profile is mirrored about its centre point),
- Deep deck profile (studied in the calibration exercise in Section 2)
- 200 mm concrete flat slab (studied in the calibration exercise in Section 2)

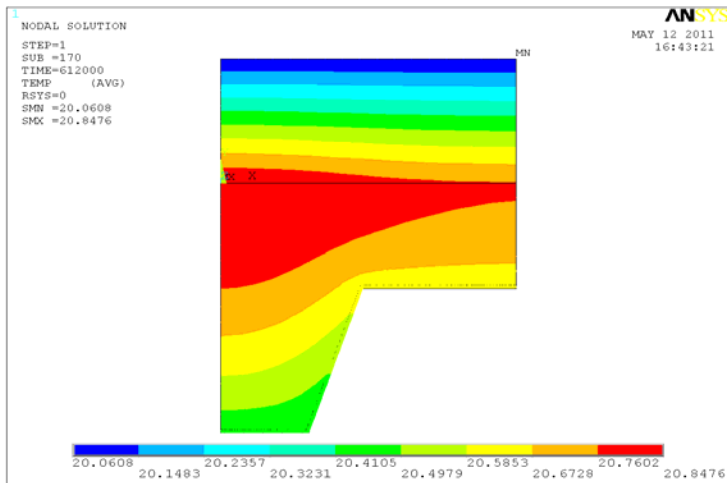
The deck thickness selected was 1.25 mm and remained constant for all thermal models created. Insulation of thickness 50 mm was used across the top surface. The material properties were those given in Table 3-1. The shape of the deep deck profile is given in Figure 3-6. The shape of the Cofraplus 60 profile is given in Figure 3-1 and the dovetail re-entrant profile dimension is the same as the Cofraplus 60 profile with the diagonal mirrored about its centre point.



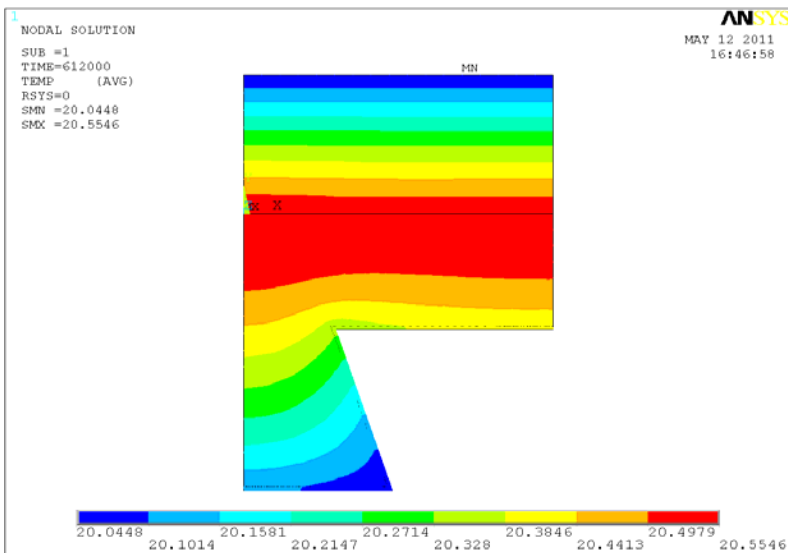
**Figure 3-6 Dimension of simplified Deep deck profile**

Figure 3-7 to Figure 3-10 show the temperature profile across the composite slab for the different profile shapes. Figure 3-11 shows the thermal flux on the bottom surface for the various deck profiles.

It can be seen from Figure 3-11 that the deep deck profile appears to produce the highest peak flux and performs the best of the four profiles chosen. However, the four profiles use different volumes of concrete - the 200 mm concrete slab contains over three times the volume of concrete compared to that of the trapezoidal profile. It was felt therefore that in order to present a more accurate representation of the “effectiveness” of the profiles to take up the applied heat load, the results should be normalised. Figure 3-12 represents the values normalised with respect to the concrete volume of the trapezoidal profile and demonstrates that the three metal decking profiles (trapezoidal, dovetail re-entrant and deep deck) perform similarly, and significantly better than the flat concrete slab.



**Figure 3-7** Temperature °C for trapezoidal deck profile at 3am. Depth of concrete from the bottom of the rib = 100mm.



**Figure 3-8** Temperature °C for dovetail deck re-entrant profile at 3am. Depth of concrete from the bottom of the rib = 100mm.

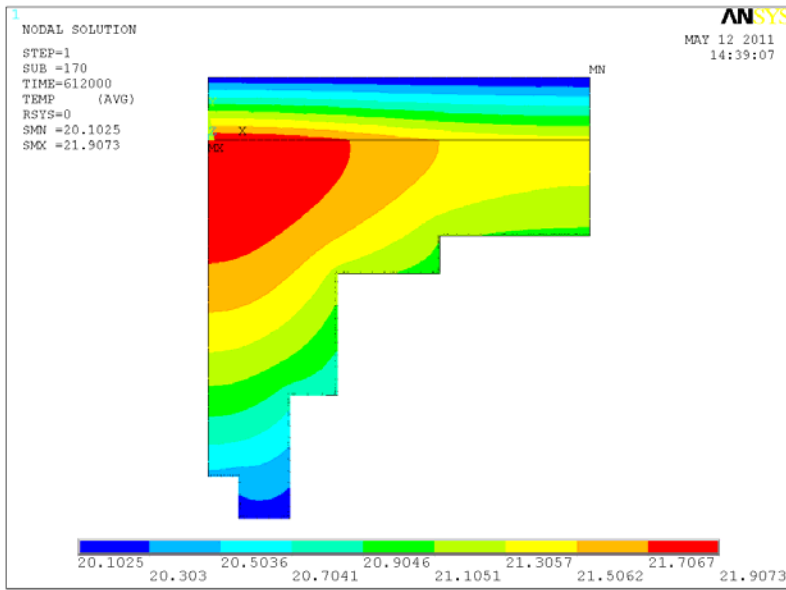


**Figure 3-9** Temperature °C for Deep deck profile at 3am. Depth of concrete from the bottom of the rib = 300mm.

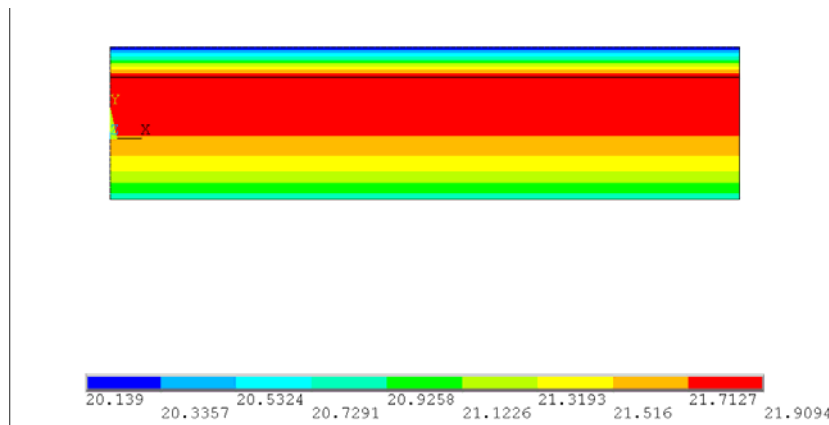


**Figure 3-10** Temperature °C for 200mm Concrete Slab at 3am.



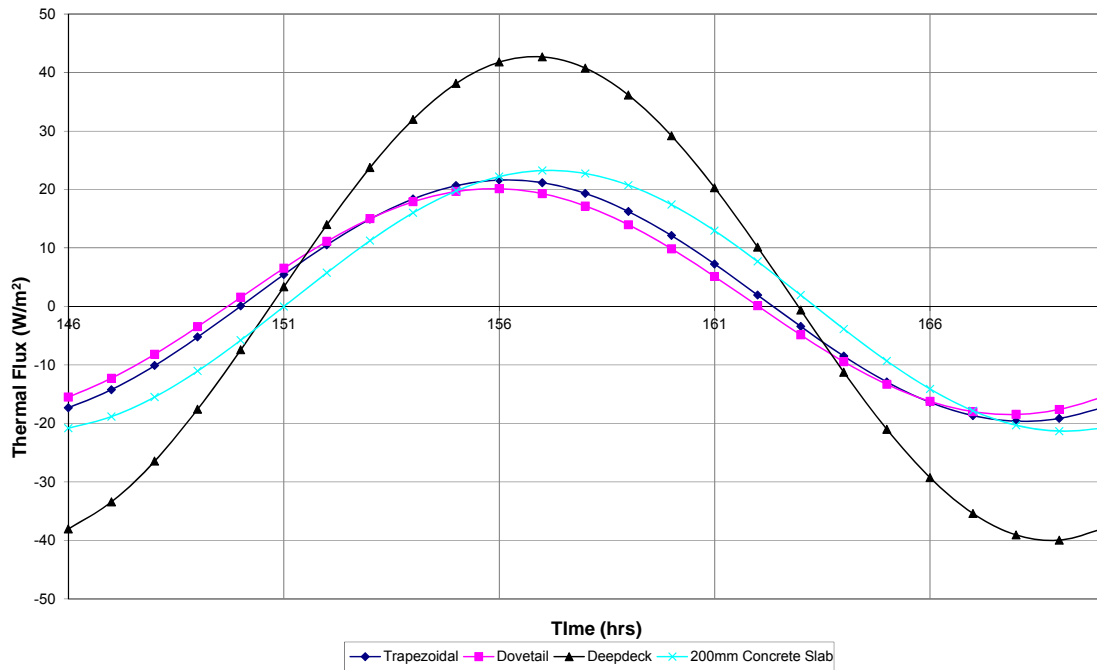


Figure 3-11 7<sup>th</sup> day thermal flux on bottom surface per horizontal metre for various deck profiles ( $W/m^2$ ).

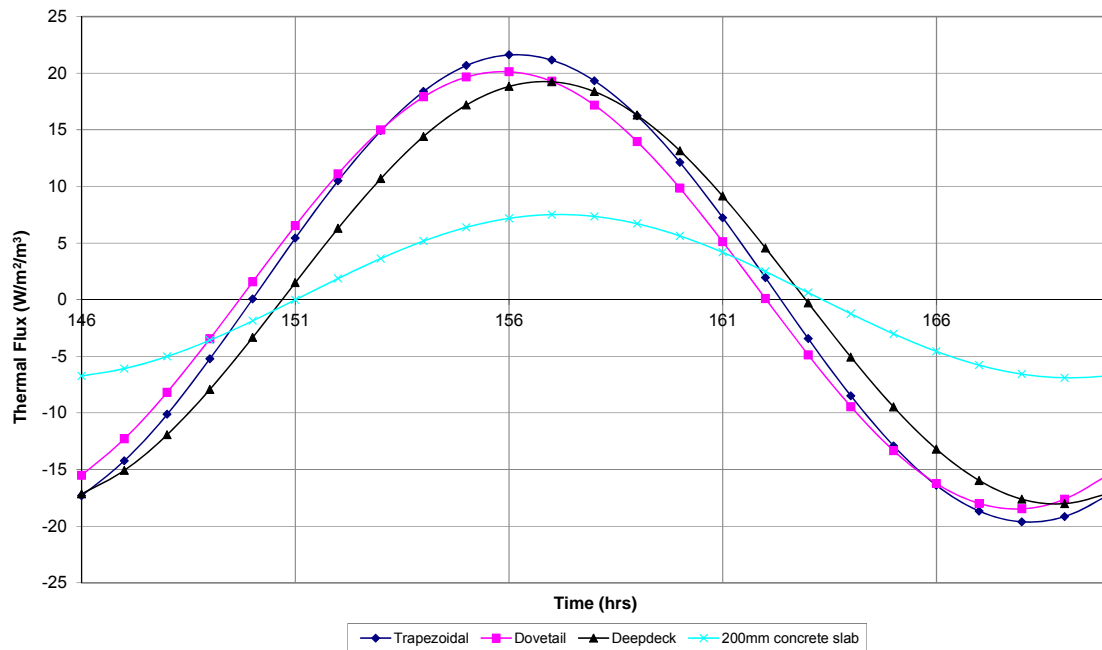


Figure 3-12 7<sup>th</sup> Day Thermal Flux on Bottom Surface per horizontal metre (Adjusted for concrete volume) for various deck profiles ( $W/m^2$ ).

### 3.5 Variation in emissivity

It was evident from the analysis performed for Section 3.2 that the emissivity ( $\varepsilon$ ) value for the surface of the metal decking has a significant impact on the quantity of heat transferred to the composite floor. It was therefore deemed necessary to investigate the effect of the emissivity value further. Seven models were developed for values of emissivity between 0.2 and 0.7. The profile for all models was as per previous models (ArcelorMittal Cofraplus 60). The deck was 1.25 mm thick for all models and had ferritic stainless steel material properties. The concrete was kept at a thickness of 100 mm for all models.

As discussed previously, it is possible for the emissivity of both galvanised steel and stainless steel to have a range between 0.075 and 0.9. This range is due to the different types of surface finish available for the two materials. The higher the value of emissivity i.e. the closer the value is to 1.0, the more effective the material is at absorbing and emitting energy. A shiny surface will be worse than a black body at absorbing and emitting heat when compared to a black body.

Figure 3-13 and Figure 3-14 show the thermal flux on the bottom surface for the different emissivity values. The results clearly show that as the emissivity ( $\varepsilon$ ) value increases, the thermal flux increases. The relationship appears to be linear and this is in line with the equation used to calculate the surface resistance and hence the film resistance<sup>[9]</sup>. It should be noted that the closer the emissivity is to unity, the duller the surface finish will appear to be. From an aesthetic point of view, it may be more desirable to have a polished finish. However, the more highly polished the finish, the less effective the surface will be at transmitting heat to the slab. In effect, the more shiny the surface of the deck, the more it will reflect heat back to the room and this is not desirable if the slab is to be used as a means of passively cooling the building space.

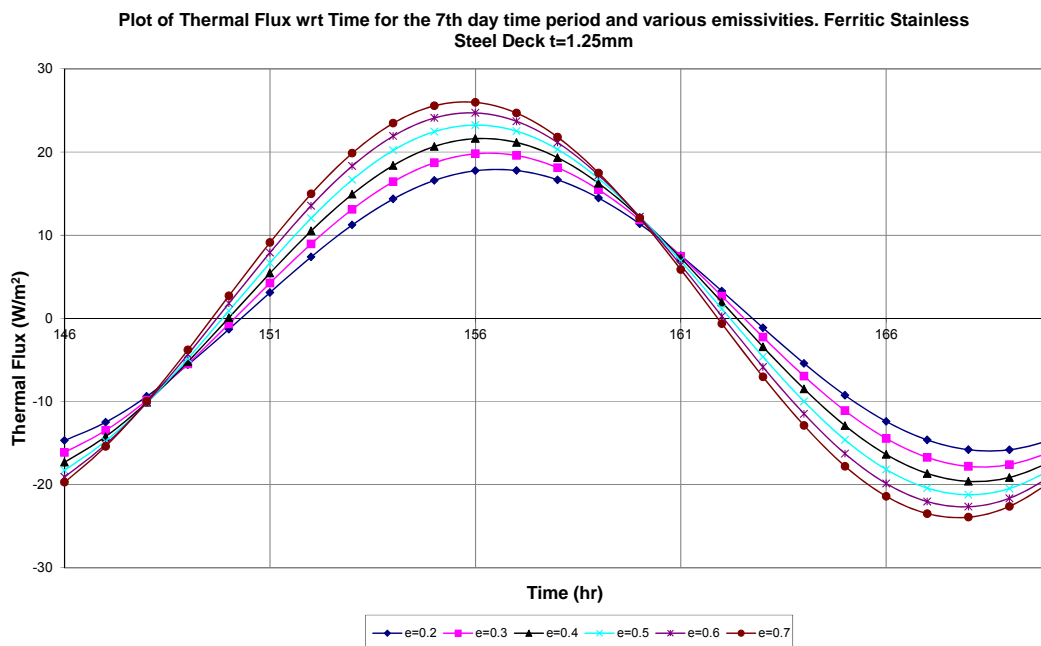


**Figure 3-13** 7th day thermal flux ( $\text{W/m}^2$ ) on bottom surface per horizontal metre for various emissivity values.

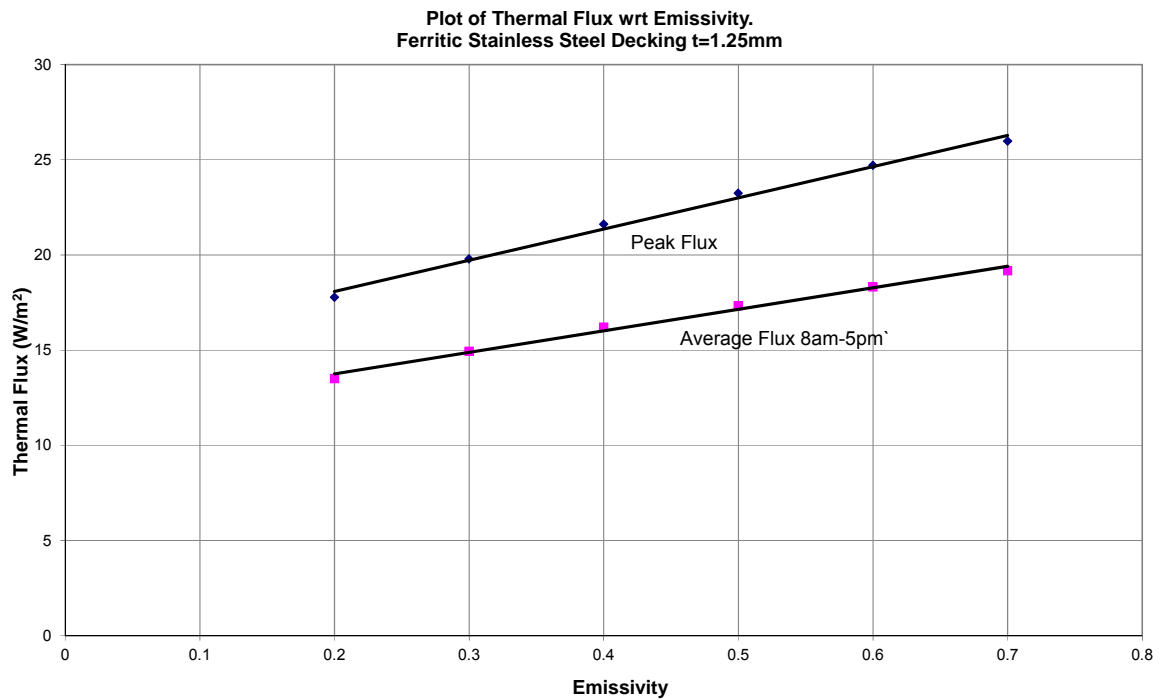


**Figure 3-14** Thermal flux (Peak & Average 8am-5pm) (W/m<sup>2</sup>) on bottom surface per horizontal metre for ferritic stainless steel deck and for various emissivity values.

## 4 IMPACT ON WHOLE BUILDING ENERGY PERFORMANCE

This section studies the impact of composite floors with ferritic stainless steel on the whole building energy performance. To do this, the results obtained from Section 3 were integrated into the simple building model outlined in Section 5.7 of the Chartered Institution of Building Services Engineers (CIBSE) Guide A Environmental Design<sup>[14]</sup>. The first step of the procedure was to calculate the thermal admittance and transmittance of the composite floor.

### 4.1 Calculation of thermal admittance and thermal transmittance

The thermal admittance of an element may be defined as the ratio of heat flow and temperature through an interior surface when the exterior temperature is 0°C. It is defined in magnitude by two terms, amplitude and a time lag. Three cases will be used for comparison; 130 mm deep composite slab with 1.25 mm thick ferritic stainless steel decking, 130 mm deep composite slab with 1.25 mm thick galvanised steel decking and a 200 mm concrete slab.

Figure 4-1, Figure 4-2 and Figure 4-3 give the input temperature and thermal flux on the underside and top surfaces of the three models. The admittance and transmittance can be calculated from the peak flux divided by the peak temperature and the lag of the peaks of the flux from the peak temperature. These values are summarised in Table 4-1.

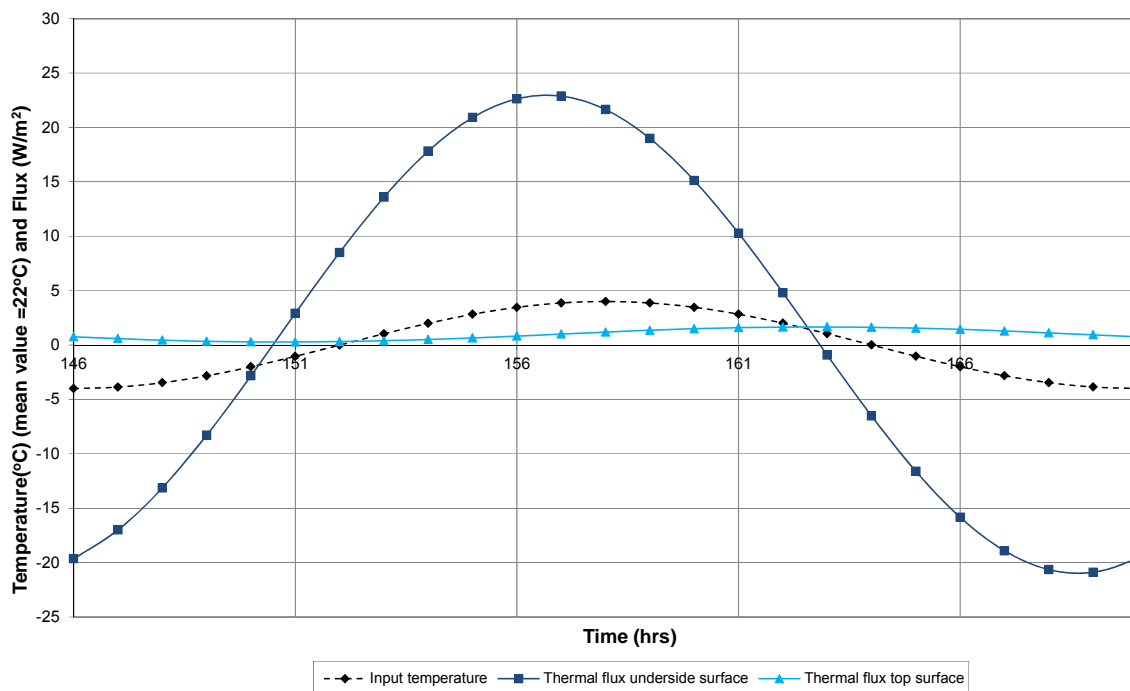


**Figure 4-1** Input temperature and thermal flux on underside and top surfaces for seventh day time period: ferritic decking

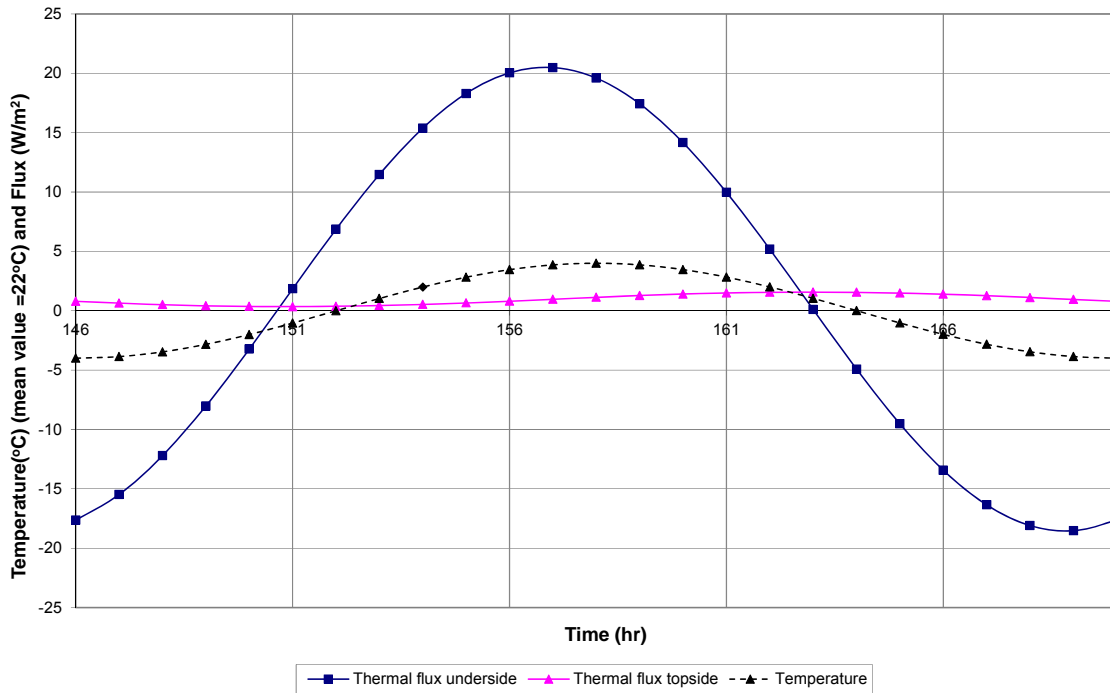


**Figure 4-2** Input temperature and thermal flux on underside and top surfaces for seventh day time period: galvanised decking

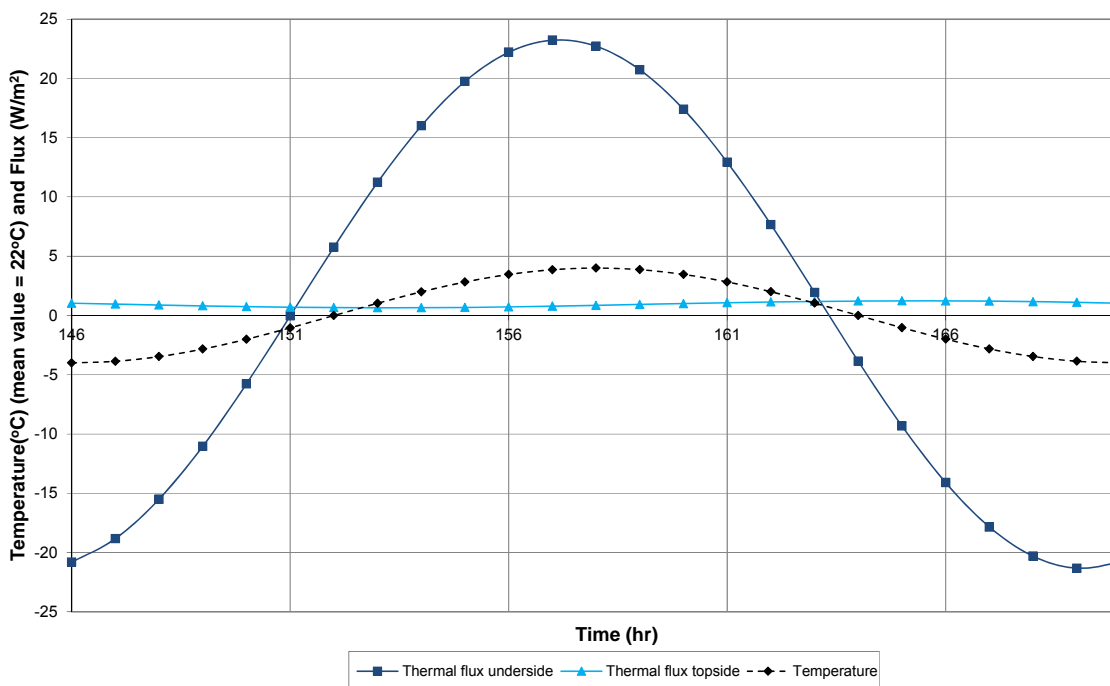


**Figure 4-3** Input temperature and thermal flux on underside and top surfaces for seventh day time period for a 200 mm thick concrete slab

**Table 4-1 Admittance, transmittance and lag values for 3 floor types**

Floor type	Depth	Admittanc	Lag	Transmittanc	Lag
	mm	W/m <sup>2</sup> K	hr	W/m <sup>2</sup> K	hr
Composite with ferritic decking	135	5.72	1	0.42	-5
Composite with galvanised	135	5.12	1	0.39	-5
200 mm concrete slab	200	5.57	1	0.31	-7

## 4.2 CIBSE simplified model

The values of admittance and transmittance obtained in Section 4.1 were used in the simplified model of a single room building as outlined in Section 5.7, example 5.2 of the CIBSE Guide A<sup>[14]</sup>. In the example, the only change made was to the admittance value (Y) of Table 4-2 and Table 4-3.

**Table 4-2 CIBSE Guide A, simplified model of a single room building**

As per CIBSE Guide							
Surface	Area	U value	(A x U)	Y	(A x Y)	Decrement	Time lag
	(m <sup>2</sup> )	Wm <sup>2</sup> /K	W/K	Wm <sup>2</sup> /K	W/K	factor f	Φ/h
External wall (opaque)	3.08	0.49	1.51	4.56	14.04	0.18	9.50
Internal wall	40.88			4.13	168.83		
Internal floor	19.80			5.31	105.14		
Ceiling (interim floor)	19.80			0.61	12.08		
Glazing (inc. frame)	7.00	2.94	20.58	3.01	21.07	1.00	0.49
<b>ΣA=</b>	<b>90.56</b>	<b>ΣAU=</b>	<b>22.09</b>	<b>ΣAY=</b>	<b>321.17</b>		
130 mm Composite slab with ferritic decking							
Surface	Area	U value	(A x U)	Y	(A x Y)	Decrement	Time lag
	(m <sup>2</sup> )	Wm <sup>2</sup> /K	W/K	Wm <sup>2</sup> /K	W/K	factor f	Φ/h
External wall (opaque)	3.08	0.49	1.51	4.56	14.04	0.18	9.50
Internal wall	40.88			4.13	168.83		
Internal floor	19.80			5.31	105.14		
Ceiling (interim floor)	19.80			5.72	113.26		
Glazing (inc. frame)	7.00	2.94	20.58	3.01	21.07	1.00	0.49
<b>ΣA=</b>	<b>90.56</b>	<b>ΣAU=</b>	<b>22.09</b>	<b>ΣAY=</b>	<b>422.34</b>		

**Table 4-3 CIBSE Guide A, simplified model of a single room building**

130 mm Composite slab with galvanised decking							
Surface	Area	U value	(A x U)	Y	(A x Y)	Decrement	Time lag
	(m <sup>2</sup> )	Wm <sup>2</sup> /K	W/K	Wm <sup>2</sup> /K	W/K	factor f	Φ/h
External wall (opaque)	3.08	0.49	1.51	4.56	14.04	0.18	9.50
Internal wall	40.88			4.13	168.83		
Internal floor	19.80			5.31	105.14		
Ceiling (interim floor)	19.80			5.12	101.38		
Glazing (inc. frame)	7.00	2.94	20.58	3.01	21.07	1.00	0.49
<b>ΣA=</b>	<b>90.56</b>	<b>ΣAU=</b>	<b>22.09</b>	<b>ΣAY=</b>	<b>410.46</b>		
200mm concrete slab							
Surface	Area	U value	(A x U)	Y	(A x Y)	Decrement	Time lag
	(m <sup>2</sup> )	Wm <sup>2</sup> /K	W/K	Wm <sup>2</sup> /K	W/K	factor f	Φ/h
External wall (opaque)	3.08	0.49	1.51	4.56	14.04	0.18	9.50
Internal wall	40.88			4.13	168.83		
Internal floor	19.80			5.31	105.14		
Ceiling (interim floor)	19.80			5.57	110.29		
Glazing (inc. frame)	7.00	2.94	20.58	3.01	21.07	1.00	0.49
<b>ΣA=</b>	<b>90.56</b>	<b>ΣAU=</b>	<b>22.09</b>	<b>ΣAY=</b>	<b>419.37</b>		

Using the values in Table 4-2 and Table 4-3, it can be seen that on calculating the thermal response factor for the three models being considered, all three fall within the scope of a 'slow response structure' (Table 5.6 of Reference 14). This means that all three buildings will have the same solar gain factor and ultimately will result in the same values being calculated for mean and the mean-to-peak swing in operative temperature. In the case of example 5.2 of Reference 14, these values are calculated as 31.51°C and 4.68 °C.

## 5 CONCLUSIONS

Thermal analysis was undertaken of composite floor slabs with ferritic stainless steel decking. Firstly the models were calibrated against earlier work on galvanised steel decking. The models were then used to study the impact of deck thickness, concrete thicknesses, profile shape and surface emissivity on thermal performance.

It was found that, when the deck thickness was varied, within reasonable limits, there was no significant increase in thermal flux across the surface. This was true for both the galvanised steel decking and the ferritic steel decking. When the concrete thickness was varied, the thermal flux increased significantly to a point. After the concrete thickness reached a certain depth (140 mm approximately), there was no significant increase in thermal flux across the bottom surface.

When the profile shape was varied, the thermal flux could vary sizeably between different profile shapes. On further investigation it was found that this was predominantly due to the different quantities of concrete used between the four profile shapes studied. When this difference in concrete volume was accounted for, it was found that the three metal deck profiles appeared to be very similar in their “effectiveness” at transferring heat to the slab. The 200 mm flat slab was found to be considerably less effective at transferring heat, primarily due to the increase in surface area given by the metal deck profiles.

When the emissivity of the surface was varied, the thermal flux changed considerably. The relationship between thermal flux on the bottom surface and the emissivity value appears to be linear, where an increase in emissivity results in an increase in the thermal flux across the bottom surface. This is consistent with the equation used to represent the radiation component of heat transferred to the slab<sup>[9]</sup>. The result may not be desirable though, because generally shiny surfaces are considered more attractive and the shinier the surface (the lower the emissivity), the less effective at transferring heat to the slab.

Integrating the values obtained for admittance and transmittance into the simplified model of the CIBSE Guide A Example 5.2, it was found that although the values of admittance and transmittance vary between a 130 mm thick slab with ferritic stainless steel decking, a 130 mm thick slab with galvanised steel decking and 200 mm concrete slab, it still resulted in the three models being categorised as having a ‘slow thermal response’. This leads to the conclusion that all three buildings will have the same solar gain factor and ultimately will result in the same values being calculated for mean and peak operative temperature. It is worth noting, however, that for both composite floor systems, despite using considerably less concrete than the 200 mm concrete slab, the resulting mean and peak operative temperatures are the same. This is due to the crudeness of the assumed model outline in CIBSE Guide A Example 5.2 where only two building classifications are allowed, a ‘slow response’ or a ‘fast response’.



## 6 RECOMMENDATIONS FOR FURTHER WORK

In the analysed models, radiation and convection were accounted for in the way described in Section 2.1 through the use of the equation obtained from Reference 9. This simplicity in modelling could be improved. In particular, Reference 9 states that in a situation where heat is flowing to and from a material, the horizontal convection coefficient can be used for all cases. This is a simplistic assumption and a more accurate value could be obtained by using varying convection coefficients for heat flow to and from the deck surface. For situations where different deck profiles were being studied, surface viewing factors will vary considerably. It may be required to apply the radiation load separately to the convection load to take the viewing factors into account. This should be investigated in future analyses, but for the purpose of this analysis the approach was deemed satisfactory.

Using the simplified CIBSE model outlined in example 5.2 of Reference 14 resulted in all the models being classified as having a 'slow thermal response' and hence being represented by identical mean and operative temperatures. The simple classification of buildings as having either a 'slow response' or a 'fast response' may be too simplistic and should be investigated in a future analysis with a more refined model.

## 7 REFERENCES

- 1 Steel Construction - Thermal Mass, The Steel Construction Institute, 2013 (available from [www.tatasteelconstruction.com](http://www.tatasteelconstruction.com))
- 2 Barnard, N and Ogden, R (1996). The thermal capacity of steel frame buildings. Seminar Paper available from the Steel Construction Institute, UK
- 3 ISO 6946 (1997). Building components and building elements - Thermal resistance and thermal transmittance -- Calculation method. International Organization for Standardisation.
- 4 Barnard, N., Concannon, P. and Jaunzens, D, BRE Information Paper IP6/01 Modelling the performance of thermal mass (2001). BRE, Watford, UK
- 5 Kendrick, C. Thermal analysis of typical composite slabs over a daily heating and cooling cycle. November 2005, Oxford Brookes University, UK
- 6 Betteridge, C.S. Determination of cyclic thermal properties: admittance, decrement factor and surface factor. Corus Research, Development and Technology. Reference Source no. 133807.
- 7 Betteridge, C.S. Determination of cyclic thermal properties of complex roof and floor constructions by finite element analysis. Corus Research, Development and Technology. Reference Source no. 133808.
- 8 EN 1994-1-2:2005 Eurocode 4. Design of composite steel and concrete structures. Part 1-2: General rules – Structural fire design, London, British Standards Institution.
- 9 BS EN 6946:2007. Building Components and Building Elements -Thermal Resistance and Thermal Transmittance - Calculation method.
- 10 EN 10088-1:2005. Stainless Steels-Part 1: List of stainless steels.
- 11 <http://www.optotherm.com/emiss-table.htm>
- 12 [http://www.thermoworks.com/emissivity\\_table.html](http://www.thermoworks.com/emissivity_table.html)
- 13 [http://www.engineeringtoolbox.com/emissivity-coefficients-d\\_447.html](http://www.engineeringtoolbox.com/emissivity-coefficients-d_447.html)
- 14 CIBSE Guide A, Environmental Design, Chartered Institution of Building Services Engineers London, 2006